Analysis and performance comparison of the trellis coded and convolutional coded DS/SSMA systems in impulsive noise environment

K.S.Kim
I.Song
S.I.Park
B.-H.Chung

Indexing terms: Trellis-coded modulation, Convolutional-coded modulation, Noise

Abstract: The authors investigate the performance of two types of direct-sequence spread-spectrum multiple-access (DS/SSMA) systems in an impulsive noise, Rician fading environment. It is observed that it is possible to get some coding gain over uncoded systems except at low SNR and that additional coding gain can be obtained by using optimum asymmetric TCM. It is also shown that the performance of the DS/SSMA systems degrades more as the noise becomes more impulsive.

1 Introduction

The demand for mobile communications is increasing rapidly, and more reliable communications are required to provide better services for the users. To achieve this, a number of modulation and coding techniques have been developed. Among these techniques, trellis-coded modulation (TCM) and convolutional coding have been investigated in such channels as the additive white Gaussian noise (AWGN), Rayleigh/Rician fading, and multiple-access channels [1–4].

It is well known that sometimes the Gaussian noise assumption cannot be entirely justified [5–7]. The non-Gaussian nature of atmospheric and various man-made noise are among the typical examples. In general, such a non-Gaussian noise tends to produce larger-magnitude observations than would be expected by a Gaussian model, and can be successfully modelled with the ε-contaminated PDF [5].

To share communication channels among multiple users, spread-spectrum multiple-access techniques have been developed. Among these techniques, direct-sequence spread-spectrum multiple access (DS/SSMA) has been a highlighted research area. In this paper, we will investigate the DS/SSMA systems using TCM and convolutional coding in an impulsive noise environment. The main advantage of TCM over convolutional coding is that it requires less bandwidth. In DS/SSMA systems, however, convolutional coding can be employed without bandwidth expansion by using shorter pseudonoise (PN) sequences. We will obtain the upper bound on the bit-error probability of the M-ary phase shift keying (PSK) trellis-coded DS/SSMA (TC-DS/SSMA) and convolutional coded DS/SSMA (CC-DS/SSMA) systems, and compare the performance of the two systems subject to the same complexity and throughput.

2 System model

The transmitter models for the TC-DS/SSMA and CC-DS/SSMA systems are illustrated in Fig. 1. The signal

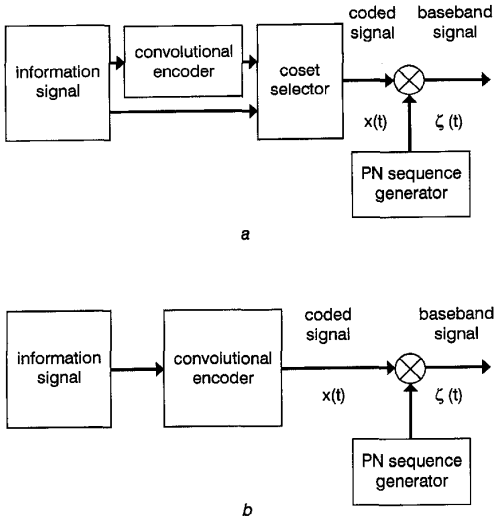

Fig. 1 *Transmitter models*
a TC-DS/SSMA system
b CC-DS/SSMA system

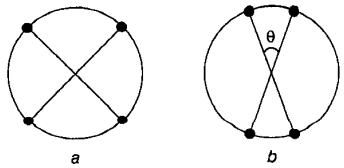

Fig. 2 *4-PSK signal constellations*
a Symmetric
b Asymmetric

IEE Proceedings online no. 19982133

Paper first received 16th September 1996 and in revised form 2nd December 1997

K.S. Kim, I. Song and S.I. Park are with the Department of Electrical Engineering, Korea Advanced Institute of Science and Technology (KAIST), 373-1 Guseong Dong, Yuseong Gu, Daejeon 305-701, Korea

B.-H. Chung is with the Mathematics Section, College of Science and Technology, Hongik University, Chochiwon 339-701, Korea

used in the CC-DS/SSMA system is the binary PSK, and the signal constellation for TCM is the 2^n-PSK: as an example, the symmetric and asymmetric 4-PSK signal constellations are illustrated in Fig. 2. The notations in the following developments are based on those in [1].

Let the kth user's complex (baseband) coded signal be

$$x^k(t) = \sum_{p=-\infty}^{\infty} x_p^k P_T(t - pT) \tag{1}$$

where T is the symbol period, P_T is a rectangular pulse of duration T, and x_p^k is the complex baseband symbol of the kth user during the pth symbol period, and is determined by the encoder and coset selector. Similarly, the PN chip signal is defined as

$$a^k(t) = \sum_{m=-\infty}^{\infty} a_m^k \Psi(t - mT_c) \tag{2}$$

where a_m^k is the mth chip of the kth user, and Ψ is the chip waveform of duration T_c. Then, the transmitted signal modulated by a carrier with frequency f_c is

$$s^k(t) = \sqrt{\frac{2E_s}{T}} \mathrm{Re}\left\{\zeta^k(t) \exp\left[j(w_c t + \psi^k)\right]\right\} \tag{3}$$

where E_s is the symbol energy, $\omega_c = 2\pi f_c$, $\zeta^k(t) = a^k(t)x^k(t)$, and ψ^k is the random phase of the kth carrier. If we assume that the fading is slowly-varying nonselective, the received signal can be written as

$$r(t) = \sqrt{\frac{2E_s}{T}} \times \mathrm{Re}\left\{\sum_{k=1}^{K} \rho^k(t)\zeta^k(t - \tau^k) \exp\left[j(w_c t + \beta^k)\right]\right\} + \eta(t) \tag{4}$$

where $\rho^k(t)$ is the fading process of the kth signal, τ^k is the random delay of the kth user at the receiver, $\beta^k = \psi^k - w_c\tau^k$ is the random phase of the kth user at the receiver, and $\eta(t)$ is impulsive noise. Here, we assume that we use coherent reception: thus, we can set τ^l and β^l in the output of the lth user's demodulator to zero.

If we assume that the fading is constant during a symbol period, the pth equivalent complex baseband sample Y_p^l of the lth user is

$$\begin{aligned} Y_p^l &= \sqrt{\frac{2}{T}} \int_{(p-1)T}^{pT} r(t)a^l(t) \exp(-j\omega_c t)dt \\ &= \sqrt{E_s}\rho_p^l x_p^l + \sqrt{E_s} z_p^l + \eta_p^l \end{aligned} \tag{5}$$

where

$$z_p^l = \frac{1}{T} \int_{(p-1)T}^{pT} \sum_{k=1, k\neq l}^{K} \rho^k(t)e^{j\beta^k} x^k(t - \tau^k) \times a^k(t - \tau^k)a^l(t)dt$$

and

$$\begin{aligned} \eta_p^l &= \eta_{pi}^l + j\eta_{pq}^l \\ &= \sqrt{\frac{2}{T}} \int_{(p-1)T}^{pT} \eta(t)a^l(t) \exp(-j\omega_c t)dt \end{aligned}$$

The impulsive noise components of the in-phase (I) and quadrature (Q) channels, η_{pi}^l, and η_{pq}^l, respectively, are zero-mean independent and identically distributed random variables with variance $Var\{\eta_{pi}^l\} = Var\{\eta_{pi}^l\} = Var\{\eta(t)\}$ and the ε-contaminated PDF [5]

$$f(x) = (1 - \epsilon)f_B(x) + \epsilon f_T(x) \tag{6}$$

where ε is a constant in [0, 1], and both the background PDF f_B and the tail PDF f_T are Gaussian with mean zero and variances σ_B^2 and $\sigma_T^2 = M\sigma_B^2$, respectively. The number M represents how much heavier the tail of f_T is than that of f_B, and ε is a parameter representing how frequently large-valued x occurs. From now on, we use the notation $\alpha(x; \varepsilon, m_f, \sigma_B^2, \sigma_T^2)$ to denote the ε-contaminated PDF (eqn. 6), with m_f the common mean of f_B and f_T. Then, the signal to noise ratio is

$$\begin{aligned} SNR &= \frac{E_s}{2E\{\eta^2(t)\}} \\ &= \frac{E_s}{2(1 + (M - 1)\epsilon)\sigma_B^2} \end{aligned} \tag{7}$$

3 Performance analysis

We now assume that the lth user is the desired user without loss of generality and drop the superscript l for convenience. Let $X_p = \sqrt{E_s}x_p$ be the pth complex coded symbol, Y_p be the corresponding complex receiver output sample, and $Z_p = \sqrt{E_s}z_p$ be the pth sample of the complex inter-user interference. Then, the pth output sample Y_p is

$$Y_p = \rho_p X_p + Z_p + \eta_p \tag{8}$$

where ρ_p is the Rician fading envelope with the PDF [8]

$$\begin{aligned} f_\rho(x) = 2x(1 + K) \exp\left[-\left\{K + x^2(1 + K)\right\}\right] \\ \times I_0\left(2x\sqrt{K(K + 1)}\right) \end{aligned} \tag{9}$$

In eqn. 9, I_0 is the zero-order modified Bessel function of the first kind, and K is the Rician parameter defined as the ratio of the energy of the direct component to that of the diffused multipath components. The work in [1] has been accomplished under the AWGN assumption: in this paper, on the contrary, we consider the impulsive noise environment.

First, we assume [9] that the inter-user interference Z_p is Gaussian, independent of η_p. Then

$$\overline{\eta}_p = Z_p + \eta_p \tag{10}$$

is also [10] ε-contaminated with PDF $\alpha(x; \varepsilon, 0, \sigma_{\bar{B}}^2, \sigma_{\bar{T}}^2)$, where $\sigma_{\bar{B}}^2 = \sigma_B^2 + \sigma_I^2$, $\sigma_{\bar{T}}^2 = \sigma_T^2 + \sigma_I^2$, $\sigma_I^2 = (Q - 1)E_s/3N$, Q is the number of users, and N is the length of the PN sequence. From now on, we drop the bars of $\overline{\eta}_p$, $\sigma_{\bar{B}}^2$, and $\sigma_{\bar{T}}^2$ for convenience.

Assume that we use a pilot tone and the estimation of the fading parameter is perfect. Then the pairwise error probability given $\rho = \{\rho_p | p \in \nu\}$ can be obtained as

$$\begin{aligned} &P(x \to \tilde{x}|\rho) \\ &= \Pr\left\{\sum_{p\in\nu}\left(\|Y_p - \rho_p X_p\|^2 - \|Y_p - \rho_p \tilde{X}_p\|^2\right) \geq 0\right\} \\ &= \Pr\left\{\sum_{p\in\nu}\left(-E_s\rho_p^2\|x_p - \tilde{x}_p\|^2\right.\right. \end{aligned}$$

$$- 2\sqrt{E_s}\rho_p \mathrm{Re}\{\eta_p(x_p - \tilde{x}_p)^*\}\Big) \geq 0\Big\} \tag{11}$$

where $\tilde{X}_p$ is the pth symbol of a coded sequence $\tilde{X} \neq X$ and ν is the set of p such that $X_p \neq \tilde{X}_p$. Now, let us define

$$\overline{d}^2 = \sum_{p\in\nu} \rho_p^2 \|d_p\|^2 \tag{12}$$

and

$$v = \sum_{p\in\nu} v_p = -\sum_{p\in\nu} (d_{pi}\rho_p\eta_{pi} + d_{pq}\rho_p\eta_{pq}) \tag{13}$$

where the pth distance $d_p = x_p - \tilde{x}_p = d_{pi} + jd_{pq}$. Then we can rewrite eqn. 11 as

$$P(x \to \tilde{x}|\rho) = \Pr\left\{-E_s\overline{d}^2 + 2\sqrt{E_s}\sum_{p\in\nu} v_p \geq 0\right\} \tag{14}$$

After some manipulations on eqn. 14 as shown in the Appendix, we get

$$P(x \to \tilde{x}|\rho) \leq (1-\epsilon)D_B^{\overline{d}^2} + \epsilon D_T^{\overline{d}^2} \tag{15}$$

The unconditional pairwise error probability bound is then obtained by taking the expectation of eqn. 15 over ρ as

$$P(x \to \tilde{x}) \leq (1-\epsilon)E\left\{D_B^{\overline{d}^2}\right\} + \epsilon E\left\{D_T^{\overline{d}^2}\right\} \tag{16}$$

and the bit-error probability bound is obtained as

$$P_b \leq (1-\epsilon)\cdot\frac{1}{2n}\left.\frac{\partial\overline{T}(D,I)}{\partial I}\right|_{D=D_B,I=1} + \epsilon\cdot\frac{1}{2n}\left.\frac{\partial\overline{T}(D,I)}{\partial I}\right|_{D=D_T,I=1} \tag{17}$$

where $\overline{T}(D, I)$ is the transfer function of the super-state diagram whose branch label gains are modified based on the discussion in [11], and the factor 1/2 is inserted based on the discussion on the error bound in [12]. Naturally, for $\varepsilon = 0$, eqn. 17 is the same as the result shown in [11].

Until now, we have not assumed whether we use trellis or convolutional code. Thus, we can obtain from eqn. 17 the upper bound of the bit-error probability of the TC-DS/SSMA system if $\overline{T}(D, I)$ is the transfer function of the TCM scheme: similarly, we can get the upper bound of the bit-error probability of the CC-DS/SSMA system.

Now, let us explain the implication of eqn. 17. At low SNR, the bit-error probability is high. If the bit-error probability is much higher than ε, the first term in the right-hand side will dominate since the second term cannot be larger than ε. At high SNR, on the other hand, the bit-error probability is low. If the bit-error probability is much lower than ε, the second term will dominate.

4 Asymmetric PSK signal constellation

In [13], it has been shown that TCM with an optimally designed asymmetric PSK (APSK) signal constellation has some gain in the bit-error probability sense over that with a symmetric PSK (SPSK) signal constellation. We can expect that TCM with an optimally designed APSK signal constellation will have a better performance than that with SPSK under an impulsive noise environment, also. With the APSK constellation in Fig. 2*b*, the transfer function is a function of θ as well as D and I.

After some steps similar to those for eqn. 17, we have

$$\begin{aligned} P_b &\leq \min_{0\leq\theta\leq\pi}(1-\epsilon)\cdot\frac{1}{2n}\left.\frac{\partial\overline{T}(D,I|\theta)}{\partial I}\right|_{D=D_B,I=1} + \epsilon\cdot\frac{1}{2n}\left.\frac{\partial\overline{T}(D,I|\theta)}{\partial I}\right|_{D=D_T,I=1} \\ &= (1-\epsilon)\cdot\frac{1}{2n}\left.\frac{\partial\overline{T}(D,I|\theta_{opt})}{\partial I}\right|_{D=D_B,I=1} + \epsilon\cdot\frac{1}{2n}\left.\frac{\partial\overline{T}(D,I|\theta_{opt})}{\partial I}\right|_{D=D_T,I=1} \end{aligned} \tag{18}$$

where $\overline{T}(D, I|\theta)$ is the transfer function of the TCM scheme with an APSK signal constellation for the fading channel. The transfer functions $\overline{T}(D, I|\theta)$ and $\overline{T}(D, I)$ can be obtained similarly, except that the branch label gains are functions of θ in $\overline{T}(D, I|\theta)$.

Now, let us explain the implication of eqn. 18. At very low SNR, the bit-error probability is much higher than ε, and the first term in the right-hand side will be the dominant factor of the bit-error probability, since the second term cannot be larger than ε. On the other hand, the bit-error probability is much lower than ε at very high SNR, and the second term will be the dominant factor, since the effect of the fact that D_B is smaller than D_T is significant at high SNR. For intermediate values of the SNR, there exists a transition from one asymptote to the other, and the value of the SNR at which the transition begins will be larger for smaller ε. Since the bit-error probability is dominated by the first and second terms at low and high SNR, respectively, we can guess that the optimum values of θ at low and high SNR are quite close to those under AWGN of variances σ_B^2 and σ_T^2, respectively. Thus we can use the results in [11, 13], where the optimum values are obtained under an AWGN environment.

5 Numerical results

To compare the performance of the convolutional and trellis coding schemes, we will assume the following: the throughput (information bit rate) of the coding schemes are fixed, the chip duration is the same for both coding schemes, and the complexity of a coding scheme is determined only by the number of states.

To set the throughputs of the rate k/n CC-DS/SSMA and TC-DS/SSMA systems equally, the PN sequence used in the CC-DS/SSMA system should be shorter by a factor of k/n than that used in the TC-DS/SSMA system. Among the convolutional codes with the same throughput, we can choose high or low rate ones: for example, we can use a rate 1/8 code with a PN sequence of period 63 as well as a rate 1/2 code with a PN sequence of period 255. It is conjectured that the performance with a lower rate convolutional code is better because of the increased distance [2]. In this paper, we will compare the rate 1/2 TC-DS/SSMA, rate 1/2 CC-DS/SSMA, rate 1/8 CC-DS/SSMA, and rate 1/2 optimum asymmetric TC-DS/SSMA systems, all with the same throughput. We further assume that the

desired signal and all interferers arrive at the receiver with the same relative power. Since the following results are obtained from the transfer function upper bounds, the real performance could be much better.

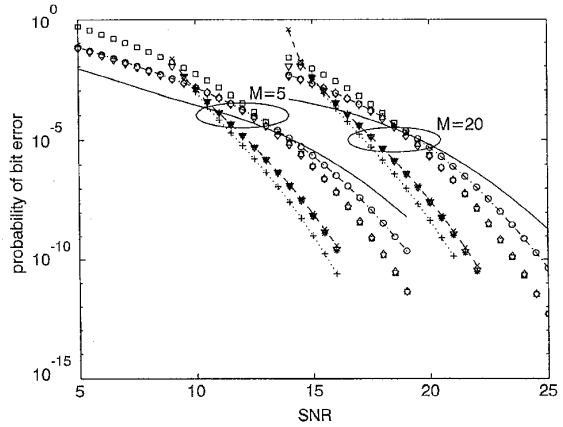

Fig. 3 *Bit error probabilities when $M = 5, 20$, $\varepsilon = 0.01$, $K = \infty$ (no fading)*

—— 1/2 2–S CC
○○○ 1/2 2–S TC
– – – – 1/2 4–S CC
××× 1/2 4–S TC
····· 1/2 8–S CC
+ + + 1/2 8–S TC
◇◇◇ 1/2 2–S asym. TC
▽▽▽ 1/2 4–S asym. TC
□□□ 1/8 2–S CC
∗∗∗ 1/8 4–S CC
—— uncoded BPSK

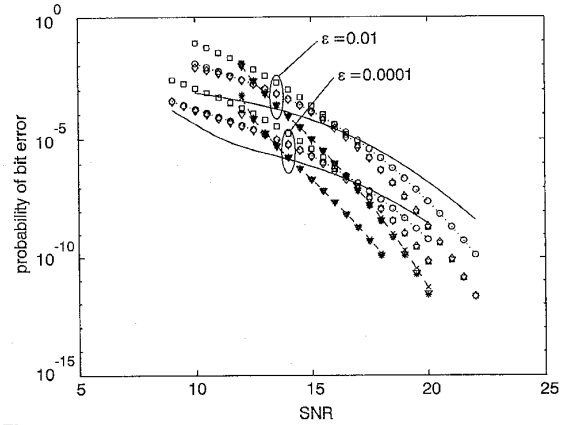

Fig. 4 *Bit error probabilities for various ε when $M = 10$ and $K = \infty$ (no fading)*

····· 1/2 2–S CC
○○○ 1/2 2–S TC
– – – – 1/2 4–S CC
××× 1/2 4–S TC
◇◇◇ 1/2 2–S asym. TC
▽▽▽ 1/2 4–S asym. TC
□□□ 1/8 2–S CC
∗∗∗ 1/8 4–S CC
—— uncoded BPSK

The bit-error probabilities of the TC-DS/SSMA and CC-DS/SSMA systems for $M = 5$, 20 are shown in Fig. 3. The number of users is 20, and the periods of the PN sequences used in the rate 1/2 TC-DS/SSMA, rate 1/2 CC-DS/SSMA and rate 1/8 CC-DS/SSMA, systems are 511, 255 and 63, respectively. We can first see that the TC-DS/SSMA and CC-DS/SSMA systems have some coding gains over the uncoded BPSK DS/SSMA system except at low SNR, and that the bit-error probabilities increase as M increases for fixed ε. The performance of the rate 1/2 TC-DS/SSMA and rate 1/2 CC-DS/SSMA systems at the same throughput and complexity is almost the same, and gets better as the complexity increases. It is also observed that the performance of the lower rate (rate 1/8) CC-DS/SSMA system is better than that of the higher rate (rate 1/2) TC-DS/SSMA and CC-DS/SSMA systems at the same throughput and complexity, as in the Gaussian noise. The performance of the optimally designed rate 1/2 asymmetric TC-DS/SSMA system is better than that of the rate 1/2 symmetric TC-DS/SSMA and rate 1/2 CC-DS/SSMA systems, and is almost the same at that of the rate 1/8 CC-DS/SSMA system. We can easily see that the gain obtained from using ATCM gets larger as the SNR increases.

The bit-error probabilities of the two systems when $M = 10$ and $\varepsilon = 0.01$, 0.0001 are shown in Fig. 4. We can see that the bit-error probabilities increase as ε increases for fixed M even at the same SNR. This result is not an unexpected one since the noise becomes more impulsive as ε increases. The bit-error probabilities of the two systems for various K when $M = 10$ and $\varepsilon = 0.01$ are shown in Fig. 5. It is natural that the performance gets worse as the fading gets more severe (K gets smaller). We can see that the gain from using optimum ATCM gets larger as the fading becomes less severe. In addition, we can make observations similar to those made for Fig. 3.

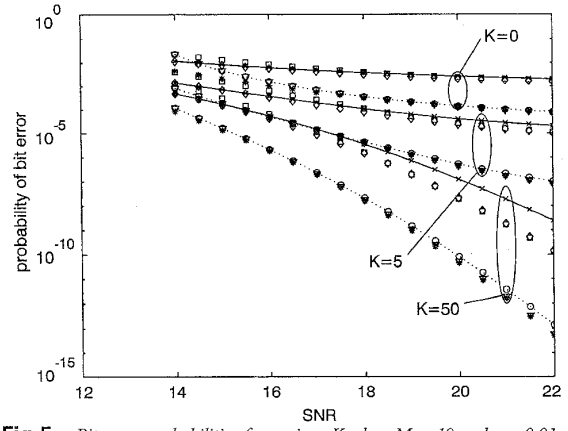

Fig. 5 *Bit error probabilities for various K when $M = 10$ and $\varepsilon = 0.01$*

—— 1/2 2–S CC
××× 1/2 2–S TC
◇◇◇ 1/2 2–S asym. TC
····· 1/2 4–S CC
○○○ 1/2 4–S TC
▽▽▽ 1/2 4–S asym. TC
□□□ 1/8 2–S CC
∗∗∗ 1/8 4–S CC

6 Conclusion

In this paper, we studied the performance of the TC-DS/SSMA and CC-DS/SSMA systems in impulsive noise, Rician fading channels. We also investigated the effect of impulsive noise on the DS/SSMA systems employing STCM, optimum ATCM and convolutional code, and compared the systems in various channel states.

From the result, it is shown that the performance of the TC-DS/SSMA and CC-DS/SSMA systems with the same throughput and complexity is almost the same, and that we can get some coding gain over uncoded systems except at low SNR. It is observed that the performance of the systems degrades more as the noise becomes more impulsive (M and ε increase). We have also seen that additional coding gain over STCM can be obtained by using optimum ATCM: the gain gets larger as the SNR increases or the fading becomes less severe.

7 Acknowledgment

This research was supported by the Korea Science and Engineering Foundation (KOSEF) under Grant 961-

0923-134-2, for which the authors would like to express their thanks.

8 References

1 BOUDREAU, G.D., FALCONER, D.D., and MAHMOUD, S.A.: 'A comparison of trellis coded versus convolutionally coded spread-spectrum multiple-access systems', *IEEE J. Sel. Areas Commun.*, 1990, **8**, pp. 628–640

2 VITERBI, A.J.: 'Very low rate convolutional codes for maximum theoretical performance of spread-spectrum multiple-access channels', *IEEE J. Sel. Areas Commun.*, 1990, **8**, pp. 641–649

3 WU, J., and LIN, S.: 'Multilevel trellis MPSK modulation codes for rayleigh fading channel', *IEEE Trans. Commun.*, 1993, **41**, pp. 1311–1318

4 PARK, S.I., KIM, K.S., KIM, H.M., and SONG, I.: 'The DS/SSMA systems using trellis coding with asymmetric PSK signal constellation', *Signal Process.*, 1998, **67**, pp. 173–187

5 KASSAM, S.A., and POOR, H.V.: 'Robust techniques for signal processing: a survey', *IEEE Proc.*, 1985, **73**, pp. 433–481

6 KASSAM, S.A.: 'Signal detection in non-Gaussian noise' (Springer-Verlag, New York, 1987)

7 PARK, S.I., LEE, K.Y., and SONG, I.: 'Performance analysis of FHSS BFSK systems with nonlinear detectors in selective fading impulsive noise environment', *Signal Process.*, 1995, **45**, pp. 275–292

8 JAMALI, S.H., and LE-NGOC, T.: 'Coded-modulation techniques for fading channels' (Kluwer Academic Publishers, Norwell, 1994)

9 PURSLEY, M.B.: 'Performance evaluation of phase-coded spread spectrum multiple-access communication-part I: system analysis', *IEEE Trans. Commun.*, 1977, **25**, pp. 795–799

10 KIM, K.S.: 'The effects of impulsive noise on the performance of DS/SSMA systems using TCM'. M.S. Thesis, KAIST, Daejeon, Korea, 1995

11 BIGLIERI, E., DIVSALAR, D., McLANE, P.J., and SIMON, M.K.: 'Introduction to trellis-coded modulation with applications' (Macmillan Publishing Company, New York, 1991)

12 SIMON, M.K., OMURA, J.K., SCHOLTZ, R.A., and LEVITT, B.K.: 'Spread spectrum communications, vol 1' (Computer Science Press, Rockville, 1985)

13 DIVSALAR, D., and SIMON, M.K.: 'Trellis coding with asymmetric modulations', *IEEE Trans. Commun.*, 1987, **35**, pp. 130–141

9 Appendix

9.1 Some properties of the ε-contaminated random variables

Property 1: Let x_1, x_2 and x_3 be independent random variables with PDFs $f_{x_i}(x) = \alpha(x; \varepsilon, 0, \sigma_{B_i}^2, \sigma_{T_i}^2)$, $i = 1, 2, 3$, where $\sigma_{B_1}^2 \leq \sigma_{B_2}^2$, $\sigma_{T_1}^2 \leq \sigma_{T_2}^2$, $\sigma_{B_3}^2 = a^2\sigma_{B_1}^2 + b^2\sigma_{B_2}^2$, $\sigma_{T_3}^2 = a^2\sigma_{T_1}^2 + b^2\sigma_{T_2}^2$, $a > 0$, and $b > 0$. Then, for sufficiently large W,

$$\Pr\{ax_1 + bx_2 \geq W\} \leq \Pr\{x_3 \geq W\} \tag{19}$$

Property 2: Let $x_0, x_1, \ldots, x_N$ be independent random variables with PDFs $f_{x_i}(x) = \alpha(x; \varepsilon, 0, \sigma_{B_i}^2, \sigma_{T_i}^2)$ $i = 0, 1, \ldots, N$, where $\sigma_{B_0}^2 = \Sigma_{i=1}^N \sigma_{B_i}^2$ and $\sigma_{T_0}^2 = \Sigma_{i=1}^N \sigma_{T_i}^2$. Then, for sufficiently large W,

$$\Pr\left\{\sum_{i=1}^{N} x_i \geq W\right\} \leq \Pr\{x_0 \geq W\} \tag{20}$$

Proofs of the above properties are in [10].

9.2 Derivation of eqn. 15

Using property 1, we have from eqn. 14,

$$\begin{aligned} P(x \to \tilde{x}|\rho) &= \Pr\left\{-E_s\bar{d}^2 + 2\sqrt{E_s}\sum_{p\in\nu} v_p \geq 0\right\} \\ &\leq \Pr\left\{-E_s\bar{d}^2 + 2\sqrt{E_s}\sum_{p\in\nu} \bar{v}_p \geq 0\right\} \end{aligned} \tag{21}$$

where $\bar{v}_p$ is a random variable with PDF $\alpha(x; \varepsilon, 0, \rho_p^2\|d_p\|^2\sigma_B^2, \rho_p^2\|d_p\|^2\sigma_T^2)$. If we let $\bar{v}$ be a random variable with PDF $\alpha(x; \varepsilon, 0, \bar{d}^2\sigma_B^2, \bar{d}^2\sigma_T^2)$, eqn. 21 becomes, by property 2,

$$P(x \to \tilde{x}|\rho) \leq \Pr\left\{-E_s\bar{d}^2 + 2\sqrt{E_s}\bar{v} \geq 0\right\} \tag{22}$$

Since the PDF of $\bar{v} = -E_s\bar{d}^2 + 2\sqrt{E_s}\bar{v}$ is easily obtained to be $\alpha(x; \varepsilon, -E_s\bar{d}^2, 4E_s\sigma_B^2\,\bar{d}^2, 4E_s\sigma_T^2\bar{d}^2)$, eqn. 22 can be rewritten as

$$\begin{aligned} P(x \to \tilde{x}|\rho) &\leq \Pr\{\hat{v} \geq 0\} \\ &= (1-\epsilon)\int_0^\infty \phi\left(x; -E_s\bar{d}^2, 4E_s\sigma_B^2\bar{d}^2\right)dx \\ &\quad + \epsilon\int_0^\infty \phi\left(x; -E_s\bar{d}^2, 4E_s\sigma_T^2\bar{d}^2\right)dx \end{aligned} \tag{23}$$

where $\phi(x; m, \sigma^2)$ is the Gaussian PDF with mean m and variance σ^2. Applying the Chernoff bound to eqn. 23, we obtain

$$\begin{aligned} P(x \to \tilde{x}|\rho) &\leq (1-\epsilon) \\ &\quad \cdot \exp\left[-E_s\bar{d}^2\lambda_1 + 2E_s\sigma_B^2\bar{d}^2\lambda_1^2\right] \\ &\quad + \epsilon \cdot \exp\left[-E_s\bar{d}^2\lambda_2 + 2E_s\sigma_T^2\bar{d}^2\lambda_2^2\right] \\ &= (1-\epsilon)D_B^{\bar{d}^2}(\lambda_1) + \epsilon D_T^{\bar{d}^2}(\lambda_2) \end{aligned} \tag{24}$$

where $D_B(\lambda_1) = \exp[-E_s\lambda_1 + 2E_s\sigma_B^2\lambda_1^2]$, $D_T(\lambda_2) = \exp[-E_s\lambda_2 + 2E_s\sigma_T^2\lambda_2^2]$, and λ_1 and λ_2 are Chernoff parameters. The optimum values of λ_1 and λ_2 and the minimum bounds D_B and D_T can be obtained to be $\lambda_{1,opt} = 1/4\sigma_B^2$, $\lambda_{2,opt} = 1/4\sigma_T^2$, $D_B = \exp[-E_s/8\sigma_B^2]$ and $D_T = \exp[-E_s/8\sigma_T^2]$. Substituting these values into eqn. 24, we get eqn. 15.